Matrix Photochemistry of Gallium and Indium Atoms (M) in the Presence of Methane: Formation and Characterization of the Divalent Species CH_3MH and Univalent Species CH_3M

Hans-Jörg Himmel,*,† Anthony J. Downs,† Tim M. Greene,† and Lester Andrews‡

Inorganic Chemistry Laboratory, University of Oxford, South Parks Road, Oxford OX1 3QR, U.K., and Department of Chemistry, University of Virginia, Charlottesville, Virginia 22901

Received November 15, 1999

IR and UV/vis spectroscopic measurements have been used to chart the reactions set in train by irradiating methane-doped argon matrices containing gallium or indium atoms, first with light having $\lambda = 200-400$ nm, and subsequently with broad-band UV−visible light. Assignments of the IR absorption bands are made and their carriers characterized on the basis of D and ^{13}C substitution and by comparison either with the vibrational properties of related molecules or with those forecast by DFT calculations. Photoexcitation at $\lambda = 200-400$ nm results in insertion of the group 13 metal atom into a C−H bond to form the angular monomethylmetal hydride molecule, CH_3MH (M = Ga, In). This product is not photostable but decomposes on exposure to radiation with $\lambda = 200-800$ nm to give the first sighting of CH_3M, the simplest organic derivative of Ga(I) and In(I) to be characterized to date. The vibrational properties of the species CH_3MH and CH_3M are compared with those of related molecules and analyzed for the light they shed on the characters of the M−C and M−H bonds.

1. Introduction

During the past decade volatile organo or hydrido derivatives of group 13 metals have attracted keen interest. In particular, the possibility of generating metals or semiconductor compounds[1,2] via chemical vapor deposition (CVD) has proved to be effective for the fabrication of epitaxially grown films of these materials. However, the number of known compounds with the potential to act as suitable precursors decreases sharply from aluminum to gallium and again from gallium to indium.[2,3] One method of access to would-be precursors, hitherto exploited only sparingly, involves insertion reactions of the metal atoms which are conveniently reconnoitred in solid inert matrices at low temperatures. For example, photoexcitation of Ga or In atoms under these conditions has been shown to result in insertion into H_2 with the formation of the corresponding dihydride HMH (M = Ga, In).[4,5] We are using a similar strategy in a systematic survey of the reactivity of Ga and In atoms toward a number of small molecules, including H_2, HCl,[6] and CO.[7] Here we report on the outcome of the photolytically induced reactions of these atoms with the smallest hydrocarbon, viz. CH_4. While some of the results derived from the IR spectra of the matrices have been outlined in a preliminary communication,[8] we present here a full account of the IR spectra and in addition report on UV/vis measurements which allow for a detailed analysis and discussion of the reactions taking place. The identities of the products have been confirmed on the basis of their IR spectra (i) by the response to D or ^{13}C substitution and (ii) by comparison with the results of density functional theory (DFT) calculations.

Hence, the primary reaction brought about under the action of UV light with wavelengths in the range 200−400 nm has been shown to involve insertion of the metal atom into a C−H bond of CH_4 to form the methylmetal hydride CH_3MH (M = Ga, In). Our findings endorse earlier reports of the matrix-isolated CH_3GaH molecule, which has been characterized previously not only by its IR[5,9] and UV−visible spectra[9] but also by its EPR spectrum.[10] An earlier report indicates that Al atoms react similarly to give the analogous product CH_3AlH.[11]

* To whom correspondence should be addressed.
† University of Oxford.
‡ University of Virginia.

(1) See, for example: O'Brien, S. C. *Chem. Soc. Rev.* **1996**, *25*, 393. Jones, A. C. *Chem. Soc. Rev.* **1997**, *26*, 101. Pogge, H. B., Ed. *Electronic Materials Chemistry: an Introduction to Device Processes and Material Systems*; Dekker: Monticello, NY, 1996. Han, W.; Fan, S.; Li, Q.; Hu, Y. *Science* **1997**, *277*, 1287. Heath, J. R.; Shiang, J. J. *Chem. Soc. Rev.* **1998**, *27*, 65.
(2) Downs, A. J., Ed. *Chemistry of Aluminium, Gallium, Indium and Thallium*; Blackie: Glasgow, U.K., 1993.
(3) Downs, A. J. *Coord. Chem. Rev.* **1999**, *189*, 59.
(4) Pullumbi, P.; Mijoule, C.; Manceron, L.; Bouteiller, Y. *Chem. Phys.* **1994**, *185*, 13.
(5) Xiao, Z. L.; Hauge, R. H.; Margrave, J. L. *Inorg. Chem.* **1993**, *32*, 642.
(6) Himmel, H.-J.; Downs, A. J.; Greene, T. M. *J. Am. Chem. Soc.*, in press.
(7) Himmel, H.-J.; Downs, A. J.; Green, J. C.; Greene, T. M. *J. Phys. Chem. A*, in press.
(8) Himmel, H.-J.; Downs, A. J.; Greene, T. M.; Andrews, L. *J. Chem. Soc., Chem. Commun.* **1999**, 2243.
(9) Lafleur, R. D.; Parnis, J. M. *J. Phys. Chem.* **1992**, *96*, 2429.
(10) Knight, L. B., Jr.; Banisaukas, J. J., III; Babb, R.; Davidson, E. R. *J. Chem. Phys.* **1996**, *105*, 6607.
(11) Parnis, J. M.; Ozin, G. A. *J. Phys. Chem.* **1989**, *93*, 1204, 1220.

10.1021/om990905p CCC: $19.00
Publication on Web 02/17/2000

Laser-ablated B,[12,13] Al,[13] Ga,[13] and In[13] atoms have also been shown to react with methane, although the precise state of the metal reagent is less clear under these conditions; there is good evidence, though, that laser-ablated B atoms yield in addition to CH_3BH the species H_2CBH_2, H_2CBH, and HBCBH.[12] Likewise with the group 2/12 metal atoms, photoexcitation can be made to generate the methane insertion product CH_3MH (M = Be,[14] Mg,[14] Ca,[14] Zn,[15] Cd,[15] Hg[15]), these being even-electron molecules with a linear C−M−H skeleton in the electronic ground state. Copper atoms also react under similar circumstances, giving CH_3CuH as the first identifiable product.[16]

In addition to the identification of CH_3MH (M = Ga, In), our studies elaborate on the photochemical channels leading to and from these molecules. Irradiation with light having $\lambda = 200-800$ nm results in photodecomposition of the divalent species to afford the first experimental evidence of the corresponding univalent derivative CH_3M. The only monomethyl compound of the group 13 metals to be detected previously in the laboratory is CH_3Al, which has been identified in the gas phase by its pure rotational spectrum,[17] by neutralization−reionization mass spectrometry (NRMS),[18] and also in a cooled jet by high-resolution resonance-enhanced multiphoton ionization (REMPI) spectroscopy.[19] Otherwise, we are largely dependent on quantum chemical methods[20−22] for whatever knowledge of CH_3Al and CH_3Ga we possess. The incentive for characterizing these molecules comes partly from their potential intermediacy in chemical vapor deposition processes starting from trivalent methylmetal compounds[1,2] and partly from the desire to gain a better understanding of the bonding in univalent organometallic compounds of the group 13 metals. Other monomethyl derivatives have been formed, typically by reactions of the appropriate metal atoms, and characterized in varying degrees of detail. They include the group 1/11 metal compounds CH_3Li,[23,24] CH_3Na,[24,25] CH_3K,[25] and CH_3Cu[16] and the group 2/12 metal compounds CH_3Be,[14] CH_3Mg,[26,27] CH_3Ca,[28] CH_3Sr,[29] CH_3Ba,[30] CH_3Zn,[26] and CH_3Cd.[31] There is some evidence to suggest that certain of these species act as carriers of the metal in planetary atmospheres.[17,26−28] Hence, there are numerous precedents inviting comparison with the hitherto uncharted molecules CH_3Ga and CH_3In.

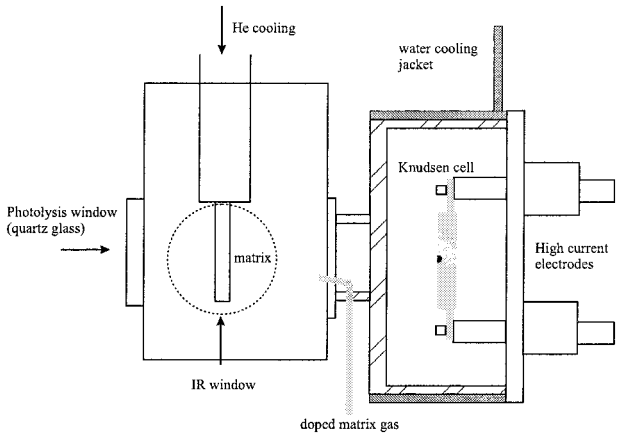

Figure 1. Schematic diagram of the matrix apparatus, including the Knudsen-type metal evaporator.

2. Experimental Section

The experiments were carried out with a newly constructed matrix apparatus incorporating a central CsI window cooled normally to 12 K by means of a Displex closed-cycle refrigerator (Air Products, Model CS202) and contained within a stainless steel vacuum shroud (see Figure 1). A turbomolecular pump (Alcatel) protected by a liquid-N_2-cooled trap was used to evacuate the assembly to a base pressure of $\leq 10^{-6}$ Torr. A water-cooled resistively heated furnace was attached to one side of the shroud; this consisted of two water-cooled electrodes separated by 5 cm and having provision for the support of a Knudsen-type cell between them. With the aid of a high-current power supply (Majestic Instruments; 400 A, 10 V), the cell could be heated to temperatures up to 2300 °C, as measured with an Re/W thermocouple.

Gallium (Aldrich, purity 99.9999%) and indium (Aldrich, purity 99.999%) were each evaporated from a tantalum Knudsen cell which was heated to 900 or 1000 °C. Hence, the vapors were deposited with an excess of methane-doped argon on the cold CsI window. The methane was admixed as supplied (BOC, Research Grade) with the argon (also BOC, Research Grade) typically at a concentration of 5%. The (Ga/In):Ar ratio was on the order of 1:600. Isotopically enriched samples of methane were also used as supplied ($^{12}CD_4$ and $^{13}CH_4$: CDN Isotopes, 99 atom % in each case). Typical deposition rates were ca. 2 mmol/h for each gas sample, continued over a period of 2−3 h. Other details of relevant equipment and procedures are given elsewhere.[15,32]

The reaction between In and methane was also investigated using laser-ablated In atoms. The fundamental 1064 nm beam of an Nd:YAG laser (Spectra Physics DCR-11) operating at 10 Hz and 20−30 mJ per pulse ablated the metal target. Further details are given elsewhere.[14]

Following deposition, the samples were exposed to the radiation from a Spectral Energy Hg−Xe arc lamp operating

(12) Hassanzadeh, P.; Hannachi, Y.; Andrews, L. *J. Phys. Chem.* **1993**, *97*, 6418. Hannachi, Y.; Hassanzadeh, P.; Andrews, L. *J. Phys. Chem.* **1994**, *98*, 6950.
(13) Jeong, G.; Klabunde, K. J. *J. Am. Chem. Soc.* **1986**, *108*, 7103.
(14) Greene, T. M.; Lanzisera, D. V.; Andrews, L.; Downs, A. J. *J. Am. Chem. Soc.* **1998**, *120*, 6097.
(15) Greene, T. M.; Andrews, L.; Downs, A. J. *J. Am. Chem. Soc.* **1995**, *117*, 8180.
(16) Parnis, J. M.; Mitchell, S. A.; García-Prieto, J.; Ozin, G. A. *J. Am. Chem. Soc.* **1985**, *107*, 8169.
(17) Robinson, J. S.; Ziurys, L. M. *Astrophys. J. Lett.* **1996**, *472*, L131.
(18) Srinivas, R.; Sülzle, D.; Schwarz, H. *J. Am. Chem. Soc.* **1990**, *112*, 8334.
(19) Clouthier, D. Unpublished results referred to in ref 20.
(20) Hoffman, B. C.; Sherrill, C. D.; Schaefer, H. F., III. *J. Mol. Struct. (THEOCHEM)* **1996**, *370*, 93.
(21) Jursic, B. S. *J. Mol. Struct. (THEOCHEM)* **1998**, *428*, 61.
(22) Fox, D. J.; Ray, D.; Rubesin, P. C.; Schaefer, H. F., III. *J. Chem. Phys.* **1980**, *73*, 3246. Jin, S. Q.; Xie, Y.; Schaefer, H. F., III. *J. Chem. Phys.* **1991**, *95*, 1834.
(23) Andrews, L.; Pimentel, G. C. *J. Chem. Phys.* **1967**, *47*, 3637. Andrews, L. *J. Chem. Phys.* **1967**, *47*, 4834.
(24) Grotjahn, D. B.; Pesch, T. C.; Xin, J.; Ziurys, L. M. *J. Am. Chem. Soc.* **1997**, *119*, 12368.
(25) Burczyk, K.; Downs, A. J. *J. Chem. Soc., Dalton Trans.* **1990**, 2351.
(26) Barckholtz, T. A.; Powers, D. E.; Miller, T. A.; Bursten, B. E. *J. Am. Chem. Soc.* **1999**, *121*, 2576.
(27) Anderson, M. A.; Ziurys, L. M. *Astrophys. J. Lett.* **1995**, *452*, L157.
(28) Anderson, M. A.; Ziurys, L. M. *Astrophys. J. Lett.* **1996**, *460*, L77.
(29) Anderson, M. A.; Robinson, J. S.; Ziurys, L. M. *Chem. Phys. Lett.* **1996**, *257*, 471.
(30) Xin, J.; Robinson, J. S.; Apponi, A. J.; Ziurys, L. M. *J. Chem. Phys.* **1998**, *108*, 2703.
(31) Panov, S. I.; Powers, D. E.; Miller, T. A. *J. Chem. Phys.* **1998**, *108*, 1335.
(32) Hawkins, M.; Downs, A. J. *J. Phys. Chem.* **1984**, *88*, 1527.

at 800 W. The first step typically involved photolysis for 10 min by UV light at wavelengths in the range 200−400 nm provided by means of a visible block filter (Oriel) which absorbed light in the range 400 < λ < 700 nm and a water filter to absorb IR radiation. This was followed by broad-band UV−visible photolysis at wavelengths in the range 200−800 nm, the output of the lamp then being transmitted only through the water filter.

Infrared spectra of the matrix samples were recorded at a resolution of 0.5 cm^{-1} and with an accuracy of ±0.1 cm^{-1} using a Nicolet Magna-IR 560 FTIR instrument equipped with a liquid-N_2-cooled MCTB detector, covering the spectral range 4000−400 cm^{-1}. UV/vis spectra were recorded in the range 300−900 nm using a Perkin-Elmer-Hitachi Model 330 spectrophotometer.

Density functional theory (DFT) calculations were performed using the GAUSSIAN98 program package[33] and applying the B3LYP method, which has been shown to give satisfactory results for small group 13 metal compounds.[21] A 6-311G(d) basis set was used for Ga; for In a LANL2DZ basis set was adopted to take into account relativistic effects.

3. Results

The infrared spectra associated with the products of the reactions of gallium and indium atoms with methane will be reported in turn. Bands have been assigned on the basis of the following criteria: (i) their response to photolysis of the matrix under different conditions as revealed by their growth/decay characteristics, (ii) comparisons with the spectra of authentic samples of a particular species or with those of related species, (iii) consideration of the selection rules expected to govern the IR activity of a given molecule, (iv) the observed effects of D or ^{13}C enrichment of the methane precursor, and (v) collation of the measured spectroscopic properties with those forecast by DFT calculations. Additionally, the UV/vis spectra of the matrices provided a means of monitoring changes in the concentration of metal atoms during the course of the reactions.

Gallium. IR Spectra. Figure 2 reproduces the IR spectra displayed by an argon matrix containing Ga atoms and CH_4 before and after photolysis. On deposition, the matrix betrayed no sign of any reaction (Figure 2a), the only features in the spectrum being those associated with unchanged CH_4 and traces of impurities (H_2O, $[H_2O]_n$, CO_2, and CO)[15] that could be reduced to a minimum but never wholly eliminated. As reported previously,[34] the H_2O gave rise to the complexes Ga···H_2O and Ga_2···H_2O, which could be identified by characteristic absorptions at 1571.9 and 1576.1 cm^{-1}, respectively.

Irradiation of the matrix with UV light having λ = 200−400 nm over a period of 10 min resulted in the appearance of new IR absorptions at 1719.7, 752.9, 528.7, and 475.5 cm^{-1} apparently belonging to the single product **1a** (Figure 2b). The most intense and distinctive features were those at 1719.7 and 752.9 cm^{-1}. Similar results have been reported earlier,[5,9] the new bands being attributed to the divalent gallium species CH_3-GaH formed by insertion of a Ga atom into a C−H bond of methane. Continued irradiation under these conditions produced little further change in the spectrum.

In contrast, after photolysis for a further 10 min, but with broad-band UV−visible light (λ = 200−800 nm), the matrix exhibited the IR spectrum depicted in Figure 2c. Hence, it was apparent that the bands due to **1a** had been totally extinguished, to be replaced by a new family of bands having a common origin in the second product **2a**. These occurred at 2986.9, 2880.2, 1403.9, 1147.9, and 476.2 cm^{-1}, the feature at lowest frequency being the most intense. Extending the period of photolysis again caused little further change in the spectrum.

The experiments were repeated using either $^{12}CD_4$ or $^{13}CH_4$ as the reagent gas; the corresponding frequencies for the normal and isotopically enriched versions of **1a** and **2a** are given in Table 1. Isotopic shifts could not be measured for all the bands associated with the two products. Evidently some features were too weak to be detected or were obscured by stronger absorptions due to other species; thus, the deuterated version of **1a** was found to exhibit one weak band at high frequency

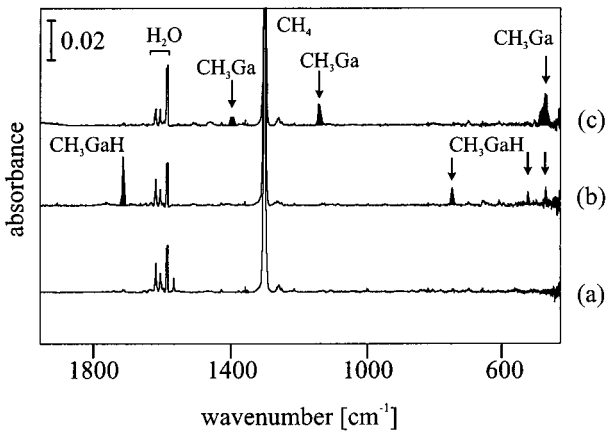

Figure 2. IR spectra recorded for an Ar matrix formed following codeposition of Ga vapor and methane: (a) after deposition; (b) after photolysis at λ = 200−400 nm for 10 min; (c) after photolysis with broad-band UV−visible light (λ = 200−800 nm) for 10 min.

Table 1. Infrared Absorptions (cm^{-1}) for the Matrix Reactions of Ga with $^{12}CH_4/^{13}CH_4/^{12}CD_4$

Ga + $^{12}CH_4$	Ga + $^{13}CH_4$	Ga + $^{12}CD_4$	<400 nm photolysis[a]	broad-band photolysis[a]	absorber
2986.9	2976.3	2200.4		↑	CH_3Ga (**2a**)
2880.2	*b*	*b*		↑	CH_3Ga (**2a**)
b	*b*	2223.9	↑	↓	CH_3GaH (**1a**)
1719.7	1719.6	1243.7	↑	↓	CH_3GaH (**1a**)
1403.9	1400.1	1025.4		↑	CH_3Ga (**2a**)
1147.9	1138.8	902.8		↑	CH_3Ga (**2a**)
752.9	748.7	578.3	↑	↓	CH_3GaH (**1a**)
528.7	516.3	*b*	↑	↓	CH_3GaH (**1a**)
476.2	464.7	*b*		↑	CH_3Ga (**2a**)
475.5	474.9	*b*	↑	↓	CH_3GaH (**1a**)

[a] Legend: ↑, increase in intensity; ↓, decrease in intensity. [b] Too weak to be observed or hidden by methane absorptions.

(33) Frisch, M. J.; Trucks, G. W.; Schlegel, H. B.; Scuseria, G. E.; Robb, M. A.; Cheeseman, J. R.; Zakrzewski, V. G.; Montgomery, J. A., Jr.; Stratmann, R. E.; Burant, J. C.; Dapprich, S.; Millam, J. M.; Daniels, A. D.; Kudin, K. N.; Strain, M. C.; Farkas, O.; Tomasi, J.; Barone, V.; Cossi, M.; Cammi, R.; Mennucci, B.; Pomelli, C.; Adamo, C.; Clifford, S.; Ochterski, J.; Petersson, G. A.; Ayala, P. Y.; Cui, Q.; Morokuma, K.; Malick, D. K.; Rabuck, A. D.; Raghavachari, K.; Foresman, J. B.; Cioslowski, J.; Ortiz, J. V.; Stefanov, B. B.; Liu, G.; Liashenko, A.; Piskorz, P.; Komaromi, I.; Gomperts, R.; Martin, R. L.; Fox, D. J.; Keith, T.; Al-Laham, M. A.; Peng, C. Y.; Nanayakkara, A.; Gonzalez, C.; Challacombe, M.; Gill, P. M. W.; Johnson, B.; Chen, W.; Wong, M. W.; Andres, J. L.; Gonzalez, C.; Head-Gordon, M.; Replogle, E. S.; Pople, J. A. GAUSSIAN 98, Revision A.3; Gaussian Inc., Pittsburgh, PA, 1998.

(34) Hauge, R. H.; Kauffman, J. W.; Margrave, J. L. *J. Am. Chem. Soc.* **1980**, *102*, 6005.

(2223.9 cm^{-1}) that lacked a counterpart in the spectrum observed for the normal molecule. Two of the bands attributed to **1a**—those at 752.9 and 528.7 cm^{-1}—experienced appreciable ^{13}C shifts, whereas large deuterium shifts characterized not only the band at 752.9 cm^{-1} but also the one at 1719.7 cm^{-1}. ^{13}C shifts ranging from 1.1 to 11.5 cm^{-1} were displayed by four of the absorptions associated with **2a**, two of which—those at 1403.9 and 1147.9 cm^{-1}—also suffered large deuterium shifts.

Apart from the main features described above, the spectra exhibited minor changes involving weak absorptions, the frequencies of which were independent of any isotopic change within the methane molecule. Accordingly, we judge these not to belong to the products of any reactions between Ga atoms and methane. Thus, the pair of bands at 1576.1 and 1571.9 cm^{-1} identifiable with the $Ga_2\cdots H_2O$ and $Ga\cdots H_2O$ adducts formed on deposition of the matrix were extinguished by irradiation at $\lambda = 200-400$ nm. In their place we witnessed the development of new bands at 1670.2 and 645.4 cm^{-1} that can be traced to HGaOH formed from the adduct by insertion of the Ga atom into one of the O−H bonds of its H_2O partner. This product also proved to be highly photolabile, being destroyed by broad-band UV−visible radiation and giving place to a product characterized by a weak band at 609.2 cm^{-1} (GaOH). The two weak absorptions observed at 1029.9 and 1001.2 cm^{-1} directly after deposition decreased following irradiation at $\lambda = 200-400$ nm and vanished completely on broad-band photolysis. They can be assigned to HGa_2OH. These products of the reactions of Ga atoms or Ga_2 dimers with water molecules have been identified in a previous matrix study.[34]

UV/vis Spectra. Prior to the studies with methane, UV/vis spectra of Ga in pure Ar matrices were examined. Figure 3 (top) shows typical UV/vis spectra of argon matrices containing Ga atoms for two different furnace temperatures (ca. 900 and 1000 °C). At the lower furnace temperature the spectrum consists of a strong absorption located around 345 nm, which was previously assigned to the $^2S \leftarrow {}^2P$ transition of Ga atoms.[9] At the higher furnace temperature the spectrum features two additional, broader absorptions with maxima at 415 and 610 nm. A band at 412 nm was previously assigned to Ga_2 and one at 610 nm tentatively attributed to higher agglomerates Ga_n.[9] Upon UV photolysis ($200 < \lambda < 400$ nm), the band associated with Ga atoms at 345 nm and that at 610 nm showed virtually no change, while the band centered at 415 nm was extinguished, presumably by irradiation into its higher energy tail. The only change observed following subsequent broad-band photolysis was a slight decrease in the intensity of the signal at 610 nm.

Figure 3 (bottom) shows the corresponding results obtained for a methane-doped matrix with the furnace at the lower temperature (ca. 900 °C). Following deposition, the strong Ga monomer absorption at 345 nm was again observed, the only difference now being a slightly enlarged half-width. Photolysis of the matrix with UV radiation ($200 < \lambda < 400$ nm) for 10 min resulted in a significant decrease of this absorption. Simultaneously, the IR spectrum witnessed the appearance of the bands attributed to species **1a**. Subsequent photolysis with broad-band UV−visible light led to the virtual extinction

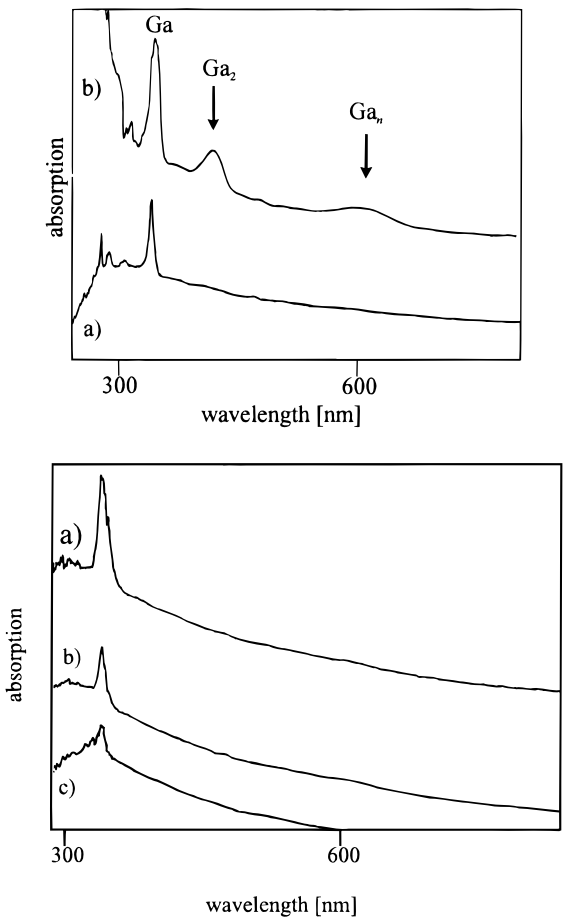

Figure 3. (top) UV/vis spectra of matrices formed by cocondensation of Ga vapor with pure argon: (a) furnace temperature ca. 900 °C; (b) furnace temperature ca. 1000 °C. (bottom) UV/vis spectra recorded for the Ar matrix formed following codeposition of Ga vapor and methane: (a) after deposition; (b) after photolysis at $\lambda = 200-400$ nm for 10 min; (c) after photolysis with broad-band UV−visible light ($\lambda = 200-800$ nm) for 10 min.

of the 345 nm band, leaving a UV/vis spectrum with no significant absorption in the range 300−900 nm, while the IR spectrum developed the features attributed to product **2a**.

Indium. IR Spectra. A set of representative IR spectra measured for an argon matrix containing In atoms and CH_4 is reproduced in Figure 4; the order of the spectra and the conditions are the same as for the gallium experiments. Once again, there was no evidence to suggest any reaction between the metal atoms and CH_4 on deposition of the matrix, the spectrum containing only the strong features associated with unchanged CH_4 and the weak ones originating in impurities (H_2O, $[H_2O]_n$, CO_2, etc.), along with the adducts $In\cdots H_2O$ and $In_2\cdots H_2O$, recognizable by absorptions at 1576.8 and 1582.9 cm^{-1}, respectively.[34]

Irradiation of the matrix at wavelengths between 200 and 400 nm for 10 min led to the appearance of new absorptions having but a single carrier, as indicated in Figure 4b. With frequencies of 1545.9 and 697.3 cm^{-1} (cf. 1719.7 and 752.9 cm^{-1}), these showed obvious affinities to the IR bands belonging to **1a** and are most plausibly ascribed to the indium analogue **1b**.

On the other hand, subsequent exposure of the matrix to broad-band UV−visible radiation ($\lambda = 200-800$ nm)

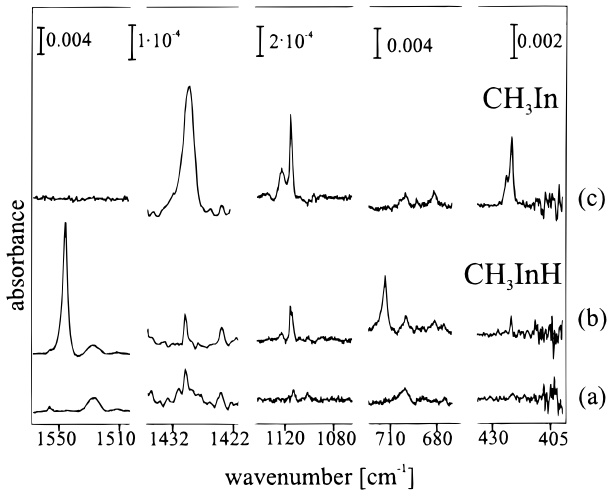

Figure 4. IR spectra recorded for an Ar matrix formed following codeposition of In vapor and methane: (a) after deposition; (b) after photolysis at $\lambda = 200-400$ nm for 10 min; (c) after photolysis with broad-band UV−visible light ($\lambda = 200-800$ nm) for 10 min.

Table 2. Infrared Absorptions (cm^{-1}) for the Matrix Reactions of In with $^{12}CH_4/^{13}CH_4/^{12}CD_4$

In + $^{12}CH_4$	In + $^{13}CH_4$	In + $^{12}CD_4$	<400 nm photolysis[a]	broad-band photolysis[a]	absorber
2976.2	*b*	*b*		↑	CH_3In (**2b**)
2905.2	*b*	*b*		↑	CH_3In (**2b**)
1545.9	1545.9	1115.0	↑	↓	CH_3InH (**1b**)
1424.0	1419.6	*b*		↑	CH_3In (**2b**)
1115.3	1107.5	868.1		↑	CH_3In (**2b**)
697.3	693.0	*b*	↑	↓	CH_3InH (**1b**)
422.1	*b*	*b*		↑	CH_3In (**2b**)

[a] Legend: ↑, increase in intensity; ↓, decrease in intensity. [b] Too weak to be observed or hidden by methane absorptions.

for 10 min brought about the extinction of the absorptions due to **1b** with the simultaneous growth of a new set of absorptions at 2976.2, 2905.2, 1424.0, 1115.3, and 422.1 cm^{-1}. The circumstances of the experiment, allied to the spectroscopic resemblance of this second product to **2a**, suggests that it is to be identified with the indium analogue **2b**.

The experiments giving rise to the products **1b** and **2b** were repeated using either $^{12}CD_4$ or $^{13}CH_4$ as the reagent gas, with the results included in Table 2. Notable aspects of **1b** were the large deuterium shift but zero ^{13}C shift of the band at 1545.9 cm^{-1} and the ^{13}C shift of 4.4 cm^{-1} of the band at 697.3 cm^{-1}. Of the bands associated with **2b**, those at 1424.0, 1115.3, and 422.1 cm^{-1} exhibited ^{13}C shifts of 4.4, 7.8, and 14.3 cm^{-1}, respectively; the only deuterium shift that could be measured satisfactorily was the substantial one suffered by the 1115.3 cm^{-1} band.

Other, weaker bands, which exhibited no shift upon isotopic substitution of the methane and therefore do not belong to a product of any reaction involving methane, included those at 1576.8 and 1582.9 cm^{-1}, which appeared on deposition of the matrix and can be assigned to the water adducts $In\cdots H_2O$ and $In_2\cdots H_2O$.[34] They disappeared after 200−400 nm photolysis, giving way to feeble signals at 1486.5 and 547.8 cm^{-1}, which can be attributed to the insertion product HInOH;[34] they were observed to vanish following broad-band photolysis. The broad feature around 915 cm^{-1} appearing

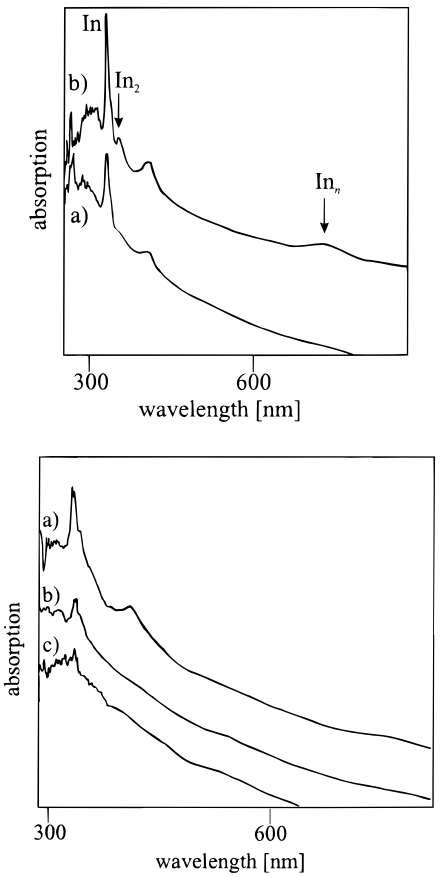

Figure 5. (top) UV/vis spectra of matrices formed by cocondensation of In vapor with pure argon: (a) furnace temperature ca. 900 °C; (b) furnace temperature ca. 1000 °C. (bottom) UV/vis spectra recorded for the Ar matrix formed following codeposition of In vapor and methane: (a) after deposition; (b) after photolysis at $\lambda = 200-400$ nm for 10 min; (c) after photolysis with broad-band UV−visible light ($\lambda = 200-800$ nm) for 10 min.

immediately after deposition belongs presumably to the insertion product of the In_2 dimer (HIn_2OH).[34] This increased after irradiation at $\lambda = 200-400$ nm but disappeared on broad-band photolysis.

Evaporation of the metal by laser ablation is likely to favor the trapping of metal atoms more than clusters and, hence, promote the formation of mononuclear metal-containing photoproducts. The results of studies involving co-deposition of laser-ablated In atoms with CH_4/Ar mixtures were noteworthy therefore for their concordance with those detailed above. IR bands due to both the products **1b** and **2b** were observed upon deposition as a result of the UV−visible radiation emanating from the metal target. The subsequent response of the products to further photolysis was as detailed above.

UV/vis Spectra. UV/vis spectra of indium vapor entrapped in an argon matrix were measured for furnace temperatures of ca. 900 and 1000 °C, with the results shown in Figure 5 (top). Evaporation at the lower temperature gave a relatively sharp absorption at 335 nm. This may be assigned to isolated In atoms previously reported to absorb at 329.4 nm.[35] In addition, a

(35) Schroeder, W.; Rotermund, H.-H.; Wiggenhauser, H.; Schrittenlacher, W.; Hormes, J.; Krebs, W.; Laaser, W. *Chem. Phys.* **1986**, *104*, 435.

Table 3. Observed and Calculated Infrared Frequencies (in cm^{-1}) for $^{12}CH_3GaH/^{13}CH_3GaH/CD_3GaD$

$^{12}CH_3GaH$		$^{13}CH_3GaH$		CD_3GaD			
obsd	calcd[a]	obsd	calcd[a]	obsd	calcd[a]	assignt	descripn of vib mode
b	3128.1 (13)	*b*	3117.1 (13)	*b*	2315.5 (4)	ν_1(a′)	ν(C−H)
b	3013.2 (12)	*b*	3009.9 (12)	*b*	2160.6 (4)	ν_2(a′)	ν(C−H)
1719.7	1730.3 (297)	1719.6	1730.3 (297)	1243.7	1233.2 (153)	ν_3(a′)	ν(Ga−H)
b	1462.7 (4)	*b*	1460.0 (3)	*b*	1058.3 (4)	ν_4(a′)	$\delta(CH_3)$
b	1219.5 (2)	*b*	1211.6 (2)	*b*	938.5 (3)	ν_5(a′)	$\delta(CH_3)$
752.9	782.0 (68)	748.7	776.9 (67)	578.3	595.8 (36)	ν_6(a′)	$\rho(CH_3)$
528.7	502.1 (25)	516.3	489.0 (25)	*b*	462.8 (21)	ν_7(a′)	ν(Ga−C)
475.5	461.1 (33)	474.9	461.0 (32)	*b*	328.5 (17)	ν_8(a′)	δ(C−Ga−H)
b	3081.5 (19)	*b*	3070.7 (19)	2223.9	2278.6 (10)	ν_9(a″)	ν(C−H)
b	1476.5 (8)	*b*	1473.4 (8)	*b*	1069.9 (4)	ν_{10}(a″)	$\delta(CH_3)$
b	598.2 (0.2)	*b*	595.1 (0.2)	*b*	447.1 (0.2)	ν_{11}(a″)	$\rho(CH_3)$
c	88.9 (1)	*c*	88.8 (1)	*c*	63.7 (0.5)	ν_{12}(a″)	$\tau(CH_3)$

[a] Symmetry C_s: C−H = 1.090 Å, C−Ga = 2.014 Å, Ga−H = 1.612 Å, ∠H−Ga−C = 118.4°, ∠H−C−Ga = 108.8°. Intensities (km mol^{-1}) are given in parentheses. [b] Too weak to be observed or hidden by methane absorptions. [c] Outside the range of detection in our experiments.

weak, broad feature near 410 nm was observed. This, together with a signal near the one at 335 nm associated with In atoms, is presumably due to the In·H_2O adduct, which was inevitably present in low concentrations. Evaporation at the higher temperature (ca. 1000 °C) gave rise to two absorptions, one at 365 nm and the other (broader) at 670 nm, in addition to those at 335 and 410 nm. The band at 365 nm is assigned to In_2 (previously reported to absorb at 375 nm when isolated in an argon matrix),[35] whereas that at 670 nm belongs most probably to higher aggregates, In_n. UV photolysis of an argon matrix containing only indium resulted in the extinction of the bands at 365 and 410 nm. The overall absorption near 335 nm decreased somewhat in intensity as a result of the photoinduced conversion of the In·H_2O adduct to HInOH. The only change on subsequent broad-band photolysis was a slight diminution in the intensity of the 670 nm band.

Figure 5 (bottom) depicts the UV/vis spectra for indium trapped in a methane-doped argon matrix following evaporation of the metal at ca. 900 °C. Following deposition, the spectrum again displayed the intense absorption at 335 nm attributable to In atoms. A weak signal at 410 nm attributable to the indium−water adduct was also observed. UV photolysis caused the band at 335 nm to decrease markedly in intensity, thereby indicating reaction of the In atoms with methane. At the same time the IR spectrum of the matrix attested to the formation of the species **1b**. Broad-band UV−visible photolysis gave no hint of recovery of the 335 nm band; instead, there was a further small decline in intensity. Meanwhile, the IR spectrum developed all the features characteristic of the species **2b**.

4. Discussion

The main infrared features observed to develop as a result of the matrix reactions induced between Ga or In atoms and methane will be shown to arise from the organometallic products CH_3MH and CH_3M (M = Ga, In). The assignments will be justified by consideration of the frequencies and isotopic shifts of the observed bands and by comparison with the vibrational properties of related species and also with the vibrational properties anticipated by DFT calculations.

CH_3MH (M = Ga, In). The product **1a**, formed by photolysis of a matrix containing Ga atoms and CH_4 at λ = 200−400 nm, is identified by the group of IR absorptions associated with it as monomethylgallium hydride, CH_3GaH, identified previously by its IR[5,9] as well as its UV−visible[9] and EPR[10] spectra. DFT calculations suggest that such a molecule has a nonlinear C−Ga−H skeleton (unlike the analogous molecules formed by the group 2/12 metals[14,15]) and so possesses C_s symmetry (see Table 3). No less than 12 infrared-active vibrational fundamentals spanning the representation 8a′ + 4a″ are therefore to be expected. Although only four of these could actually be observed in our experiments, their relative intensities, frequencies, and isotopic shifts were found to be in excellent agreement with the properties predicted for the optimized ground state of CH_3GaH by DFT/B3LYP calculations (see Table 3). Hence, we have succeeded in locating all the fundamental bands calculated to have intensities in excess of 20 km mol^{-1}. Our findings and conclusions also tally closely with those of the earlier study carried out under comparable conditions, but with higher concentrations of methane, by Lafleur and Parnis (LP);[9] in fact, LP succeeded in observing some additional, weaker absorptions, which they attributed to fundamentals of methylgallium hydride in one isotopic form or another.

The highest frequency we can thus assign to CH_3GaH on the basis of our results, coming at 1719.7 cm^{-1}, corresponds without doubt to the ν(Ga−H) mode. It compares with values of 1799.5/1727.7 and 1669.5 cm^{-1} in $HGaH$[4,5] and HGaOH,[34] respectively. The frequency of the corresponding ν(Ga−D) mode gives an H:D ratio of 1.3827:1, in keeping with a motion primarily involving the hydrogen atom (cf. the corresponding mode of CH_3ZnH, where the ratio is 1.3877:1). Of the fundamentals involving the internal motions of the CH_3Ga fragment, only those arising from the a′ CH_3 rocking and a′ Ga−C stretching modes were observed, these being calculated to be among the four most intense features in IR absorption. The location of $\rho(CH_3)$ (a′) at 752.9 cm^{-1} (supported by both the ^{13}C and deuterium shifts) may be compared with the mean value of 755 cm^{-1} found for the corresponding modes of $(CH_3)_3Ga$.[36] The substantial ^{13}C shift of the band at 528.7 cm^{-1} signals its origin in what is essentially the ν(Ga−C) mode. The frequency is comparable with, but somewhat lower than, the mean value of 561 cm^{-1} reported for the

(36) McKean, D. C.; McQuillan, G. P.; Duncan, J. L.; Shephard, N.; Munro, B.; Fawcett, V.; Edwards, H. G. M. *Spectrochim. Acta, Part A* **1987**, *43*, 1405.

Table 4. Observed and Calculated Infrared Frequencies (in cm^{-1}) for $^{12}CH_3InH/^{13}CH_3InH/CD_3InD$

$^{12}CH_3InH$		$^{13}CH_3InH$		CD_3InD			
obsd	calcd[a]	obsd	calcd[a]	obsd	calcd[a]	assignt	descripn of vib mode
b	3161.1 (19)	*b*	3150.2 (20)	*b*	2338.4 (6)	$\nu_1(a')$	ν(C−H)
b	3026.9 (32)	*b*	3024.1 (33)	*b*	2167.6 (13)	$\nu_2(a')$	ν(C−H)
1545.9	1562.2 (269)	1545.9	1562.6 (269)	1115.0	1110.5 (139)	$\nu_3(a')$	ν(In−H)
b	1472.9 (5)	*b*	1469.8 (5)	*b*	1068.5 (6)	$\nu_4(a')$	$\delta(CH_3)$
b	1219.3 (5)	*b*	1212.0 (5)	*b*	930.8 (7)	$\nu_5(a')$	$\delta(CH_3)$
697.3	756.0 (103)	693.0	751.6 (102)	*b*	570.8 (58)	$\nu_6(a')$	$\rho(CH_3)$
b	452.2 (16)	*b*	439.2 (14)	*b*	418.5 (15)	$\nu_7(a')$	ν(In−C)
b	414.4 (49)	*b*	414.3 (50)	*b*	294.9 (23)	$\nu_8(a')$	δ(C−In−H)
b	3121.7 (26)	*b*	3111.1 (27)	*b*	2307.2 (12)	$\nu_9(a'')$	ν(C−H)
b	1486.7 (9)	*b*	1483.1 (9)	*b*	1079.6 (6)	$\nu_{10}(a'')$	$\delta(CH_3)$
b	623.2 (5)	*b*	620.0 (5)	*b*	463.8 (3)	$\nu_{11}(a'')$	$\rho(CH_3)$
c	37.9 (6)	*c*	36.8 (5)	*c*	26.6 (3)	$\nu_{12}(a'')$	$\tau(CH_3)$

[a] Symmetry C_s: C−H = 1.095 Å, C−In = 2.181 Å, In−H = 1.782 Å, ∠H−Ga−C = 117.9°, ∠H−C−Ga = 109.1°. Intensities (km mol^{-1}) are given in parentheses. [b] Too weak to be observed or hidden by methane absorptions. [c] Outside the range of detection in our experiments.

Table 5. ν(M−H) and ν(M−C) Frequencies (cm^{-1}) and Stretching Force Constants (N m^{-1}) for Divalent Compounds CH_3MH and HMOH

molecule	ν(M−H)	ν(M−C)	ref	k(M−H)	k(M−C)
CH_3BeH	2062.3, 2059.4	854[a]	14	241.5	258.1
CH_3MgH	1560.3, 1552.2	539	14	140.8	161.5
CH_3CaH	1263, 1254, 1245		14	91.5	
CH_3ZnH	1866.1	564.9	15	203.9	230.7
CH_3CdH	1760.5	505.4	15	182.6	199.7
CH_3HgH	1955.3	533.9	15	225.2	235.3
CH_3BH	2680[a]	1040[a]	12	410.3	421.8
CH_3AlH	1764, 1746	610	11	176.3	214.3
HAlOH	1743.3		34	175.8	
CH_3GaH	1719.7	528.7	*b*	173.1	219.2
HGaOH	1669.8		34	163.2	
CH_3InH	1545.9	452.2[a]	*b*	140.9	160.2[a]
HInOH	1486.3		34	130.1	

[a] Calculated value. [b] This work.

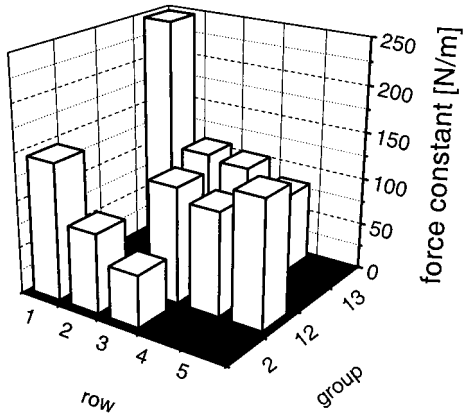

Figure 6. M−H stretching force constants for CH_3MH compounds of group 2, 12, and 13 elements.

ν(Ga−C) modes in $(CH_3)_3Ga$.[36] The final feature to be assigned to CH_3GaH and lying at 475.5 cm^{-1} is associated with the skeletal bending vibration δ(C−Ga−H), on the grounds of its minimal ^{13}C shift. Curiously LP also observed this feature but, being unable to reconcile it with a fundamental of CH_3GaH, they were obliged to associate it with an unidentified product.[9]

Hence, we begin with strong circumstantial evidence for believing that the product **1b** formed under similar conditions in a matrix containing In atoms and CH_4 is the indium analogue CH_3InH. DFT calculations point to an equilibrium structure for this molecule closely akin to that of the gallium compound with the vibrational properties detailed in Table 4. In practice, however, we were able to establish with confidence the existence of only two of the 12 infrared-active fundamentals, the others being for the most part either too weak to be detected or hidden by the stronger absorptions of other species. It proved impossible to increase significantly the concentration of this product, which appeared to be somewhat photolabile even at wavelengths in the range 200−400 nm; attempts to limit the photolyzing radiation to a narrower band-pass were frustrated by the resulting reduction in overall throughput of light. Nevertheless, the two bands clearly belonging to **1b** have all the right credentials to be assigned to the two fundamentals of CH_3InH, which are expected to be most intense in infrared absorption. The frequency, intensity, and response to isotopic change leave little doubt that the stronger band, occurring at 1545.9 cm^{-1}, represents the fundamental ν(In−H) (H:D ratio 1.3865:1). The frequency compares with values of 1615.6/1548.6 and 1486.3 cm^{-1} for the ν(In−H) modes in HInH[4] and HInOH,[34] respectively. On similar grounds, the feature at 697.3 cm^{-1} finds a plausible assignment in the a′ $\rho(CH_3)$ fundamental; the corresponding modes of $(CH_3)_3In$ have a mean frequency of 712 cm^{-1}.[37]

With the observation and partial characterization of CH_3GaH and CH_3InH, four species of this type have now been authenticated for the group 13 elements on the strength of matrix-isolation experiments,[5,9−12] although the spectroscopic details are still relatively sparse for the boron and indium compounds. It is appropriate, therefore, to take stock of the trends presented by this series of divalent molecules, particularly with regard to the properties of the M−H and M−C bonds. Table 5 summarizes the M−H and M−C stretching frequencies and force constants k for such molecules, where M is taken from either group 2/12 or group 13; M−H stretching frequencies and force constants are also included for the HMOH compounds of Al, Ga, and In. With regard to HMX molecules at large, where X = H, Me, OH, the following conclusions may then be drawn: (i) for a given element M k_{MH} varies but little with the nature of X and is close in magnitude to k_{MC} when X = CH_3, (ii) k_{MH} and k_{MC} follow the same pattern of dependence on the nature of M, varying in the order B ≫ Al ≈ Ga > In (see Figure 6), and (iii) for elements M that are horizontally related in the periodic table k_{MH}

(37) *Gmelin Handbook of Inorganic and Organometallic Chemistry*, 8th ed.; Springer-Verlag: Berlin, Heidelberg, Germany, 1991; Organoindium Compounds 1; pp 6−7.

Table 6. Geometries of HMH and CH_3MH Compounds of Group 13 Elements (Bond Lengths in Å, Bond Angles in deg)

species	∠C−M−H	*r*(M−H)	*r*(M−C)	ref
CH_3BH	127	1.19	1.56	12
HAlH	118.2	1.609		4
CH_3GaH	118.4	1.612	2.014	*a*
HGaH	117.6	1.616		4
CH_3InH	117.9	1.782	2.181	*a*
HInH	120.6	1.815		4

[a] This work.

varies in the order group 12 (e.g. Zn) > group 13 (e.g. Ga), but group 13 (e.g. Al) > group 2 (e.g. Mg). These features reflect the irregular buildup of the atomic core of M, notably through the intervention of the 3d shell, and the similarity of H and CH_3 as ligands, as well as changes of orbital overlap and polarity in the M−H and M−C bonds. Table 6 includes information about the geometries of the molecules CH_3MH (with M being a group 13 metal) drawn largely from quantum chemical calculations. The CH_3MH molecules formed by the group 13 elements, unlike those formed by the group 2/12 elements, are thus seen to have angular skeletons with ∠C−M−H on the order of 120°, the odd electron occupying an a′ orbital.

CH_3M (M = Ga, In). Irradiation with broad-band UV−visible light (λ = 200−800 nm) results in the efficient conversion of CH_3GaH to the new product **2a**, which lacks any spectroscopic sign of a Ga−H bond but evidently retains a coordinated CH_3 group. The obvious inference is that **2a** is the simple methylgallium(I) molecule, CH_3Ga, formed by photodissociation of the Ga−H bond and expulsion of a hydrogen atom which is enabled by its small size to escape from the matrix cage (eq 1).

$$CH_3M^{\bullet}H \xrightarrow[\substack{\lambda = 200-800\ \text{nm}\\ M = Ga,\ In}]{h\nu} CH_3M + H^{\bullet} \qquad (1)$$

DFT calculations find an equilibrium geometry with C_{3v} symmetry for the CH_3Ga molecule. There are therefore six distinct infrared-active vibrational fundamentals spanning the representation $3a_1 + 3e$. Our experiments located IR absorptions with relative intensities, frequencies, and isotopic shifts in close accord with those predicted here and elsewhere[20,21] by quantum chemical calculations for five of the fundamentals (see Table 7). The only missing feature, ν_6(e), is likely to lack the intensity to be detected under the conditions of our experiments.

The highest frequency band to be attributed to CH_3Ga, occurring at 2986.9 cm^{-1} and with an H:D ratio of 1.3574:1, is an obvious candidate for the antisymmetric C−H stretching mode, ν_4(e). The signal at 2880.2 cm^{-1} can be assigned to the corresponding symmetric ν(C−H) mode, $\nu_1(a_1)$. Next in order of decreasing frequency come two bands in the range 1100−1450 cm^{-1} normally associated with $\delta(CH_3)$ fundamentals. Their frequencies and response to isotopic change are as follows: 1403.9 cm^{-1}, H:D = 1.3691:1, ^{13}C shift 3.8 cm^{-1}; 1147.9 cm^{-1}, H:D = 1.2715:1, ^{13}C shift 9.1 cm^{-1}. Hence, there can be little doubt that the 1403.9 cm^{-1} band originates in $\delta_{asym}(CH_3)$ (ν_5(e)) and the 1147.9 cm^{-1} band in $\delta_{sym}(CH_3)$ ($\nu_2(a_1)$). The mean frequencies for the corresponding modes in $(CH_3)_3Ga$ are ca. 1440 and 1207 cm^{-1}, respectively.[36] The assignment of the metal−carbon stretching mode, $\nu_3(a_1)$, to the remaining absorption at 476.2 cm^{-1} is guided by its substantial ^{13}C shift (11.5 cm^{-1}) and by the suggestion of $^{69}Ga/^{71}Ga$ splitting amounting to ca. 0.8 cm^{-1}. The frequency is then substantially lower than the mean (561 cm^{-1}) for the analogous modes of $(CH_3)_3Ga$,[36] and there appears to be a progressive decrease in the order $\nu(Ga^{III}-C) > \nu(Ga^{II}-C) > \nu(Ga^{I}-C)$. A similar sequence is found for the hydrides GaH_3,[38] GaH_2,[4] and GaH.[4] Indeed, we may gain a rough estimate of the whereabouts of the ν(Ga−C) mode in CH_3Ga by scaling that of the diatomic molecule GaH[4] by the ratio of the mean frequencies of ν(Ga−C) and ν(Ga−H) in the Ga(III) species GaH_3[38] and $(CH_3)_3Ga$.[36] The result is a value of 451 cm^{-1}, in reasonable agreement with the observed frequency of 476.2 cm^{-1}.

Analogy with the photochemistry of the Ga/CH_4 system combines with the infrared spectrum carried by the indium product **2b** to argue strongly that **2b** is methylindium(I), CH_3In, formed by photodissociation of the In−H bond in the CH_3InH precursor (eq 1). DFT calculations give an optimized geometry resembling closely that of the gallium compound and having the vibrational properties listed in Table 8. In this case also our experiments appear to have hit on five of the six fundamentals, the only absentee being an absorption attributable to the CH_3 rocking mode, $\rho(CH_3)$, which is anticipated in any case to be unusually weak in infrared absorption. Information about the isotopomers CD_3In and $^{13}CH_3In$ is unfortunately less ample, partly because we were unable to secure such high concentrations and partly because of the masking effects of other absorptions. In general terms, however, the experimental results approximate closely the properties computed by DFT methods.

Two bands are observed at frequencies >2900 cm^{-1}, and the obvious interpretation is to attribute the higher frequency feature (at 2976.2 cm^{-1}) to the antisymmetric ν(C−H) mode, ν_4(e), and the lower frequency one (at 2905.2 cm^{-1}) to its symmetric counterpart, $\nu_1(a_1)$. The assignment of the features at 1424.0 and 1115.3 cm^{-1} to $\delta_{asym}(CH_3)$ (ν_5(e)) and $\delta_{sym}(CH_3)$ ($\nu_2(a_1)$), respectively, is wholly persuasive on the grounds of frequency, relative intensity, response to isotopic change, calculated properties, and analogy with CH_3Ga. This leaves only the low-frequency band at 422.1 cm^{-1}, which on the evidence of its ^{13}C shift and of the DFT-simulated properties is most obviously associated with the ν(In−C) mode, $\nu_3(a_1)$. The frequency is thus appreciably lower than that of the comparable mode in CH_3InH (ca. 450 cm^{-1}) or than the mean of the two distinct ν(In−C) modes in $(CH_3)_3In$ (486 cm^{-1}).[37] It may also be compared with the rough estimate of 394 cm^{-1} based on ν(In−H) for InH[4] and InH_3[38] and $\nu(In-C)_{mean}$ for $(CH_3)_3In$.[37] Potential uncertainty arises from the knowledge that the bending mode of InOH occurs at 421.8 cm^{-1}.[34] However, InOH can be eliminated as the carrier of the 422.1 cm^{-1} band on the grounds of (i) the marked ^{13}C shift and (ii) the absence of any detectable absorption at 522.8 cm^{-1} attributable to ν(In−O).[34]

(38) Pullumbi, P.; Bouteiller, Y.; Manceron, L.; Mijoule, C. *Chem. Phys.* **1994**, *185*, 25.

Table 7. Observed and Calculated Fundamental Frequencies for CH_3Ga (in cm^{-1})

$^{12}CH_3Ga$		$^{13}CH_3Ga$		CD_3Ga			
obsd	calcd[a]	obsd	calcd[a]	obsd	calcd[a]	assignt	descripn of vib mode
2880.2	2978.3 (22)	*b*	2977.3 (23)	*b*	2138.4 (5)	$\nu_1(a_1)$	$\nu_{sym}(C-H)$
1147.9	1223.2 (21)	1138.8	1215.4 (18)	902.8	948.5 (36)	$\nu_2(a_1)$	$\delta_{sym}(CH_3)$
476.2	472.0 (73)	464.7	459.8 (70)	*b*	432.3 (57)	$\nu_3(a_1)$	$\nu(Ga-C)$
2986.9	3049.5 (67)	2976.3	3040.7 (67)	2200.4	2254.8 (36)	$\nu_4(e)$	$\nu_{asym}(C-H)$
1403.9	1459.6 (33)	1400.1	1457.1 (33)	1025.4	1057.5 (17)	$\nu_5(e)$	$\delta_{asym}(CH_3)$
b	498.7 (7)	495.7	494.1 (7)	*b*	373.1 (4)	$\nu_6(e)$	$\rho(CH_3)$

[a] Calculation for singlet $CH_3{}^{69}Ga$. Symmetry C_{3v}: C−H = 1.101 Å, Ga−C = 2.049 Å, ∠H−C−Ga = 111.7°. Intensities (km mol^{-1}) are given in parentheses. The rms deviation of observed from calculated frequencies is 3.7%. [b] Too weak to be observed or hidden by methane absorptions.

Table 8. Observed and Calculated Fundamental Frequencies for CH_3In (in cm^{-1})

$^{12}CH_3In$		$^{13}CH_3In$		CD_3In			
obsd	calcd[a]	obsd	calcd[a]	obsd	calcd[a]	assignt	descripn of vib mode
2905.2	2989.1 (53)	*b*	2986.3 (54)	*b*	2141.5 (17)	$\nu_1(a_1)$	$\nu_{sym}(C-H)$
1115.3	1220.2 (42)	1107.5	1212.3 (39)	868.1	936.6 (49)	$\nu_2(a_1)$	$\delta_{sym}(CH_3)$
422.1	425.9 (53)	407.7	413.8 (50)	*b*	392.0 (41)	$\nu_3(a_1)$	$\nu(In-C)$
2976.2	3086.5 (78)	*b*	3076.1 (80)	*b*	2279.4 (38)	$\nu_4(e)$	$\nu_{asym}(C-H)$
1424.0	1475.0 (38)	1419.6	1471.6 (38)	*b*	1071.3 (22)	$\nu_5(e)$	$\delta_{asym}(CH_3)$
b	533.1 (0.1)	*b*	530.6 (0.1)	*b*	397.7 (0.1)	$\nu_6(e)$	$\rho(CH_3)$

[a] Calculation for singlet $CH_3{}^{115}In$. Symmetry C_{3v}: C−H = 1.103 Å, In−C = 2.226 Å, ∠H−C−In = 111.5°. Intensities (km mol^{-1}) are given in parentheses. The rms deviation of observed from calculated frequencies is 5.7%. [b] Too weak to be observed or hidden by methane absorptions.

Table 9. ν(M−C) and $\delta_{sym}(CH_3)$ Frequencies (in cm^{-1}) and CH_3−M Stretching Force Constants (N m^{-1}) for CH_3M Compounds

molecule	ν(M−C)	$\delta_{sym}(CH_3)$	$k(CH_3-M)$	ref
CH_3Li	*a*	1158	78[b]	23
CH_3Na	298	1092	47.6	25
CH_3K	275	1053	48.4	25
CH_3Be	851.7	1179	274.9	14
CH_3Mg	*a*	1072	116[b]	26
CH_3Ca	*a*	*a*	113[b]	26
CH_3Zn	445	1064	143	26
CH_3Cd	*a*	*a*	99.0[b]	31
CH_3B	*a*	*a*	354.3[b]	12
CH_3Al	*a*	*a*	184.8[b]	21
CH_3Ga	476.2	1147.9	165.3	*c*
CH_3In	422.1	1115.3	158.4	*c*

[a] Not observed. [b] Value estimated from quantum chemical calculations. [c] This work.

Table 10. M−C Bond Distances (in Å) in CH_3M Compounds of the Group 13 Elements

species	r(M−C)	ref
CH_3B	1.554[a]	12
CH_3Al	1.994[b]	17
CH_3Ga	2.049[a]	this work
CH_3In	2.226[a]	this work

[a] Value estimated by quantum chemical calculations. [b] Value determined from the rotational spectrum of the gaseous molecule.

The newly characterized molecules CH_3Ga and CH_3In invite comparison with other homoleptic monomethylmetal compounds CH_3M, where M is drawn from groups 1, 2/12, or 13. Tables 9 and 10 assemble such data about these molecules as are currently available from experimental or theoretical sources. Features of particular interest include the frequencies of the vibrational modes $\delta_{sym}(CH_3)$, ν(M−C), and $\rho(CH_3)$ and the M−C stretching force constant k_{MC} (also displayed graphically in Figure 7). For those molecules which have been identified experimentally, the frequency of $\delta_{sym}(CH_3)$ (in cm^{-1}) varies as follows: CH_3Be (1179)[14] > CH_3Li (1158)[23] > CH_3Ga (1148) > CH_3In (1115) > CH_3Na (1092)[25] > CH_3K (1053).[25] This trend can be

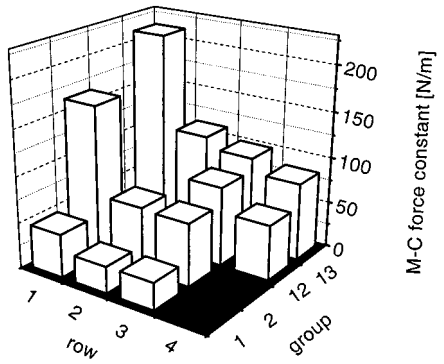

Figure 7. M−C stretching force constants for several CH_3M compounds of group 1, 2, 12, and 13 elements.

interpreted, at least in part, in terms of an increasing charge separation between the metal and methyl group. Accordingly, the metal-to-carbon bond is at its most covalent in CH_3Be and at its most polar in CH_3K. Gallium and indium clearly occupy a position intermediate between Be and the heavier group 1 elements but not far removed from lithium and sodium, respectively, in the implied polarity of the M−C bond. M−C stretching frequencies span a much wider range—from an estimated value of 978 cm^{-1} for CH_3B[12] to 275 cm^{-1} for CH_3K.[25] When these results are translated into force constants k_{MC}, we observe the pattern illustrated in Figure 7. Hence, it is evident that k_{MC} decreases as we descend each group, with the most dramatic change occurring as usual between the elements in the first and second short periods. Within a given period there is a significant increase in the order group 1 < group 2/12 < group 13. Changes in orbital overlap and bond polarity are presumably the main factors at work here. One of the most telling variations is revealed, however, by the methyl rocking mode, $\rho(CH_3)$, although it has been observed experimentally in comparatively few instances. For CH_3B the mode is calculated to come at about 600 cm^{-1}:[12] for matrix-isolated CH_3K,[25] at the other extreme, it is observed to come at 307 cm^{-1}.

Scheme 1. Reaction Pathways for the Photoactivated Matrix Reactions between Ga or In (M) and CH_4

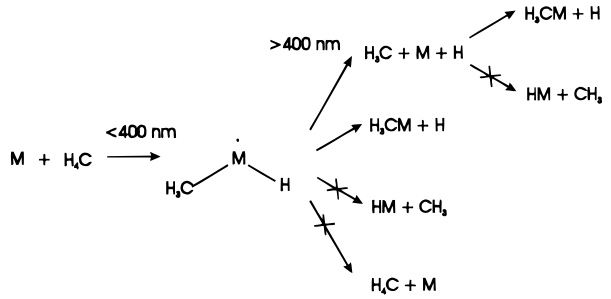

Within a particular group the frequency diminishes as a function of increasing atomic number; within a particular period it increases in the order group 1 < group 2/12 ≈ group 13. For the idealized ion pair $CH_3^-M^+$ the frequency of the motion must tend to zero, and so increasing pliability of the CH_3M assembly with respect to the $\rho(CH_3)$ coordinate reflects principally a growing separation of charge between the CH_3 and M units. This motion typically defines the line of least resistance when the molecule is exposed to outside interactions (as in aggregation or complexation, for example), which may give rise to distortion of the original CH_3M geometry. In summary, all the signs are that CH_3Ga and CH_3In carry relatively polar M−C bonds, with the indium compound being appreciably more polar than the gallium one (in keeping with the electronegativities of the two elements).

Reaction Pathways. Scheme 1 illustrates the reaction scheme inferred from our investigations of the matrix photochemistry of gallium or indium atoms in the presence of methane; in all essential respects the two metals behave in the same way under the conditions employed here. In common with others,[5,9] we find no evidence that the metal atoms in their ^2P ground electronic state (or indeed simple aggregates such as Ga_2 and In_2 also present in the matrices) undergo any reaction with methane. The same is true of Al atoms,[11] despite the fact that P-state metal atoms are found elsewhere to insert spontaneously into a C−H bond of methane and the likelihood that the reaction 2 is slightly exothermic in the case where M = Al ($^2P_{1/2}$). On the assumption that M−C bond energies are similar to M−H bond energies, and using the best estimates of these and the C−H bond energy in CH_4,[11,39,40] we deduce that reaction 2 is likely to be thermally neutral for M

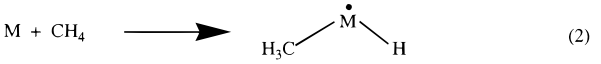

(2)

= Ga and endothermic by about 14 kcal for M = In, when each of these atoms is in its ground electronic state. Irrespective of whether the insertion reaction of the ground-state metal atom is symmetry-forbidden, as has been argued by Ozin et al.,[11] atomic gallium and indium are likely to be less reactive than aluminum.

Gallium atoms isolated in an argon matrix are reported to show absorptions at ca. 270 and 350 nm attributable to the $^2D \leftarrow {}^2P_{1/2}$ and $^2S \leftarrow {}^2P_{1/2}$ transitions, respectively.[9,41] We could clearly trace the 350 nm absorption in our UV/vis spectra but were unable to observe the 270 nm one because of the absorption of the CsI windows in our apparatus. The corresponding transitions for indium atoms occur near 330 and 400 nm, although the second transition is reported to be strongly quenched by an Ar matrix environment.[35] Radiation at wavelengths between 200 and 400 nm should therefore populate both the ^2S and ^2D excited electronic states for each of the metal atoms, for which reaction 2 becomes strongly exothermic to extents estimated to exceed 50 kcal. Despite the evidence of calculations indicating that atoms in S states are subject to highly repulsive interactions opposing side-on approach to a C−H or H−H bond,[42] earlier experiments make it clear that more or less efficient reaction occurs between the following reagents: Al (^2S) + CH_4 in matrices;[11] Ga (^2S) + CH_4 in matrices[9] and in the gas phase;[43] M (^2S) + H_2 in matrices (M = Al, Ga, In).[4] None of the studies reported to date finds any significant difference in reactivity between the ^2S and ^2D states of a given atom. Indeed, it is possible that the chemistry observed in both the present and earlier studies originates in the same M (^2S) + X potential energy surface (where M = Al, Ga, In, and X = H_2, CH_4), $^2D \leftarrow {}^2P$ excitation being followed by efficient transfer from the M (^2D) to the M (^2S) surface.[11] The behavior of the ^2D state is also clouded to some extent by overlapping of the $^2D \leftarrow {}^2P$ atomic transition and one or more transitions associated with metal aggregates.[9] The most likely explanation for what appears to be direct insertion of M (^2S) into a C−H or H−H bond is then offered by the mediation of a weakly bound but fairly specific M (^2S)···X complex. The resulting interaction may impart some attractive character to the ^2S surface, for example by admitting some mixing of the surfaces derived from the ^2S and ^2D states, and/or the complex may be sufficiently long-lived to absorb a second photon and so gain access to higher excited states with more than enough energy to overcome the normal ^2S barrier to insertion.

The matrix-isolated CH_3AlH molecule is reported to exhibit two optical absorptions, viz. at 270 and 525 nm.[11] Photolysis at 270 nm is said to result mainly in "fragmentation to form secondary products", whereas photolysis at wavelengths >450 nm results in the efficient regeneration of Al atoms, presumably through the reversal of the insertion reaction. In neither case does the infrared spectrum of the matrix give any hint of a reaction leading to the formation of the aluminum-(I) compound CH_3Al. In an earlier study LP have ascribed an optical absorption at ca. 600 nm to matrix-isolated CH_3GaH.[9] Here, too, irradiation at $\lambda > 450$ nm is said to cause the quantitative regeneration of the metal atoms, together presumably with methane. The corresponding IR spectra showed no evidence for the formation of methyl radicals. This is surprising, since Cu and methane gave evidence for the photogeneration

(39) Downs, A. J.; Pulham, C. R. *Chem. Soc. Rev.* **1994**, *23*, 175.
(40) O'Neill, M. E.; Wade, K. In *Comprehensive Organometallic Chemistry*; Wilkinson, G., Stone, F. G. A., Abel, E. W., Eds.; Pergamon Press: Oxford, U.K., 1982; Vol. 1, Chapter 1.
(41) Ammeter, J. H.; Schlosnagle, D. C. *J. Chem. Phys.* **1973**, *59*, 4784. Grinter, R.; Stern, D. R. *J. Mol. Struct.* **1982**, *80*, 147.
(42) See for example: Castillo, S.; Ramirez-Solis, A.; Diaz, D.; Poulain, E.; Novaro, O. *Mol. Phys.* **1994**, *81*, 825.
(43) Mitchell, S. A.; Hackett, P. A.; Rayner, D. M.; Flood, M. *J. Chem. Phys.* **1987**, *86*, 6852.

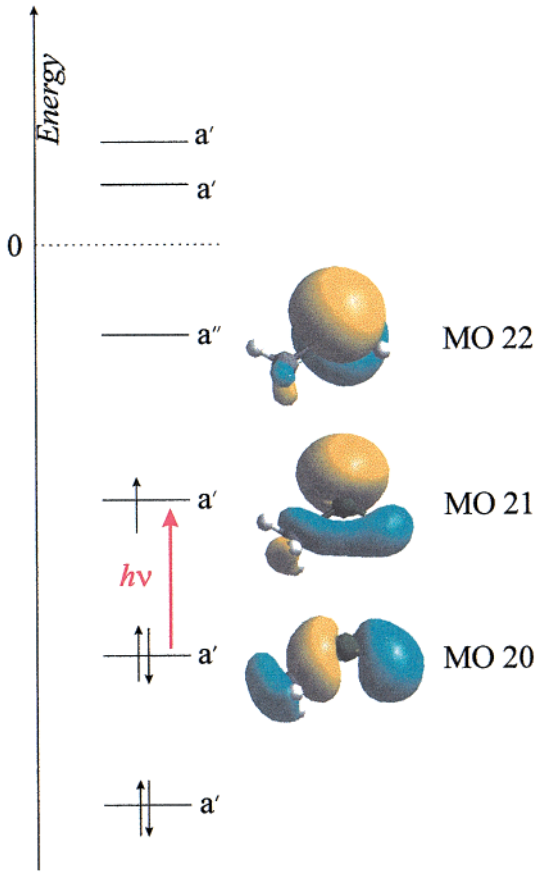

Figure 8. Outer-sphere orbitals of CH_3GaH.

of methyl radicals under analogous conditions.[16] In any event, the UV/vis spectra reported here gave no hint of recovery of the Ga atom absorption near 350 nm on broad-band UV−visible photolysis. Under the conditions applied in this study, therefore, CH_3GaH exhibits no significant decomposition to Ga atoms and methane. Instead, the IR spectra clearly indicate decomposition to CH_3Ga.

Under broad-band UV−visible irradiation (with $200 < \lambda < 800$ nm) we observe within minutes the extinction of the IR bands due to CH_3MH and their replacement by the features characteristic of CH_3M. There is no hint of the spectroscopic signatures associated with either the $CH_3^•$ radical[44] or the MH molecule.[4] Moreover, our UV/vis spectra give no reason to believe that metal atoms are regenerated. Further experiments showed as well that a second period of UV irradiation ($\lambda = 200-400$ nm) did not restore the IR absorptions of CH_3MH once they had been destroyed by broad-band photolysis. The broad-band conditions may then give access to a transition in CH_3MH, resulting in specific cleavage of the M−H bond to form CH_3M and $H^•$ atoms, as in eq 1, or in cleavage of both M−H and M−C bonds with the initial formation of M atoms together with $CH_3^•$ and $H^•$. In the second case, confinement within the matrix cage promotes recombination of the M atoms with the $CH_3^•$ radicals but not with the $H^•$ atoms, possibly because the unusual mobility of the latter allows them easy egress from the cage. Circumstantial evidence favors specific cleavage of the M−H bond. Quantum mechanical calculations were carried out to assess the outer shell orbitals of CH_3MH. Figure 8 shows plots of the electron density for the molecular orbitals 20, 21, and 22. Orbital 20 hosts two electrons, 21 has a single electron, and 22 is the LUMO. Orbital 22, consisting mainly of the 4p orbital of the Ga atom perpendicular to the molecular plane, is not involved in the bonding. Orbitals 20 and 21 result mainly from the interaction between the other two 4p orbitals of Ga with the s orbital of H and a 2p orbital of the C atom. Orbital 20 is bonding with respect to both the M−C and the M−H units. Orbital 21 has a high electron density on the metal atom with almost no electron density along the M−C and M−H axes. The lowest energy electronic transition of CH_3MH is likely to involve promotion of an electron from orbital 20 to orbital 21. The calculations predict a required wavelength of 417 nm for this excitation, and the characters of the two orbitals are consistent with decomposition of the CH_3MH in consequence, without obviously discriminating between M−C and M−H bond cleavage. It seems likely, therefore, that the matrix cage enclosing the CH_3MH molecule plays a critical part in directing the course of photodissociation.

5. Conclusions

A study of the reaction between gallium or indium atoms and methane molecules has been carried out using the technique of matrix isolation to trap the products and investigate their photochemistry. The various molecules have been identified and characterized by their infrared spectra. The conditions of the experiments, the infrared spectra of the matrices—including those of matrices containing CD_4 or $^{13}CH_4$—and comparison either with the spectra of known species or with spectra simulated by DFT calculations all testify that the metal atoms in their excited ^2S or ^2D states insert into one of the C−H bonds of methane to form the odd-electron monomethylmetal hydride species CH_3MH (M = Ga, In). These M(II) derivatives suffer photodissociation under the action of broad-band UV−visible light ($\lambda = 200-800$ nm), not with the regeneration of the metal atom and CH_4, as reported for CH_3AlH and CH_3GaH under visible light,[9,11] but with the formation of the monomethylmetal(I) compound, CH_3M. The properties deduced by experiment and theory for molecules of the types CH_3MH and CH_3M are compared with those of related species and discussed in relation to the nature of the bonds. Hence, it appears that the M−C and M−H stretching force constants vary with the valence state of M in the order M(I) < M(II) < M(III), reflecting primarily the decreasing metal−ligand charge separation. Consideration is given to the pathways taken (i) by the metal insertion process, in which a specific complex $M^*\cdots CH_4$ is probably implicated, and (ii) by the photodissociation of the insertion product CH_3MH to $CH_3M + H^•$ induced by broad-band UV−visible light.

Acknowledgment. We thank (i) Prof. J. C. Green for help with some of the calculations, (ii) the EPSRC for support of this research and for the award of an Advanced Fellowship to T.M.G., and (iii) the Deutsche Forschungsgemeinschaft for the award of a postdoctoral grant to H.-J.H.

OM990905P

(44) Milligan, D. E.; Jacox, M. E. *J. Chem. Phys.* **1967**, *47*, 5146.